

## ARTICLE OPEN



# Immobilization of active ammonia-oxidizing archaea in hydrogel beads

Matthieu Landreau<sup>1</sup>✉, HeeJun You<sup>1</sup>, David A. Stahl<sup>1</sup> and Mari K. H. Winkler<sup>1</sup>

Ammonia-oxidizing archaea (AOA) are major players in the nitrogen cycle but their cultivation represents a major challenge due to their slow growth rate and limited tendency to form biofilms. In this study, AOA was embedded in small (~2.5 mm) and large (~4.7 mm) poly(vinyl alcohol) (PVA)—sodium alginate (SA) hydrogel beads cross-linked with four agents (calcium, barium, light, or sulfate) to compare the differences in activity, the diffusivity of nitrogen species ( $\text{NH}_4^+$ ,  $\text{NO}_2^-$ , and  $\text{NO}_3^-$ ), and polymer leakage in batch systems over time. Sulfate-bound PVA-SA beads were the most stable, releasing the lowest amount of polymer without shrinking. Diffusion coefficients were found to be 2 to 3 times higher in hydrogels than in granules, with ammonium diffusivity being ca. 35% greater than nitrite and nitrate. Despite a longer lag phase in small beads, embedded AOA sustained a high per volume rate of ammonia oxidation compatible with applications in research and wastewater treatment.

npj Clean Water (2021)4:43; <https://doi.org/10.1038/s41545-021-00134-1>

## INTRODUCTION

Ammonium-oxidizing archaea are one of the most dominant clades of mesophilic and thermophilic Thaumarchaeota. Present in terrestrial, marine, and geothermal ecosystems, they play a key role in the global nitrogen cycle. Their presence in activated sludge reactors<sup>1</sup> and wastewater treatment plants<sup>2</sup>, also suggests that they participate in the removal of ammonium along with their bacterial counterparts. In the oxygen minimum zones (OMZ), AOA pairs with anaerobic ammonium oxidizing bacteria, contributing up to 50% of the N loss of the oceans<sup>3</sup>. AOA exerts primary control over ammonia oxidation at unusually low ammonia and oxygen concentrations by converting ammonium into nitrite under a wide range of temperatures (up to 74 °C)<sup>4</sup> and pH values as low as 4<sup>5</sup>. This lifestyle is close to the thermodynamic edge of net energy gain resulting in low microbial yields and growth rates<sup>3</sup>. With the isolation of the first AOA, *Nitrosopumilus maritimus*, new opportunities opened up to explore the physiology and biotechnological potential of this exceptional archaeal group<sup>6</sup>. However, due to their slow growth and poor capacity to form biofilms, they are difficult to enrich and study in continuously fed reactor systems where retention and product inhibition are a challenge<sup>7,8</sup>.

One approach to increasing cellular retention time is the use of cell immobilization as previously applied in the food, pharmaceutical, and environmental fields. Immobilization methods include the adsorption or attachment of cells to inert surfaces, self-aggregation of cells by flocculation, and cell entrapment in polymer gels or other types of matrix material<sup>9</sup>. Among available techniques, cellular entrapment of active cells in hydrogels formed by crosslinking a synthetic polymer matrix is of well-documented general utility<sup>10</sup>. Hydrogels allow the diffusion of small molecules that sustain cellular activity and growth while retaining cells in a stable network. As a consequence, hydrogels offer several advantages over suspended growth systems, including high cell density, prevention of washout, ease of solid/liquid separation, reusability, and protection of cellular integrity by the matrix material<sup>11</sup>. Cell entrapment in hydrogels has been used to develop advanced wastewater treatment technologies and to study complex microbial ecosystems, including those of the gut and hydrothermal vents. Thus, this method of cell immobilization

appears extensible to most types of microorganisms and microbial communities<sup>9,12–14</sup>. While polymers such as polyethylene glycol<sup>15–17</sup> or cellulose<sup>18</sup> have been investigated for immobilizing nitrifying microorganisms, polyvinyl alcohol is generally preferred<sup>19–24</sup> owing to its low toxicity, high porosity, high mechanical stability, low cost, and ease to use<sup>25</sup>. Poly(vinyl alcohol) (PVA) is often used in combination with sodium alginate (SA), together forming a robust gel (PVA-SA hydrogel) that resists shear forces that may occur in continuously mixed systems<sup>26</sup> such as wastewater treatment plants.

So far, applications to wastewater treatment have focused on the immobilization of ammonia-oxidizing bacteria (AOB) from enrichments<sup>21,23,27</sup> or from nitrifying activated sludge, where AOB was paired with anaerobic ammonium oxidizing (Anammox) bacteria<sup>28–31</sup> for enhanced autotrophic nitrogen removal from warm and ammonia laden sidestream wastewater. Anammox technology can reduce energy requirements by half<sup>32</sup> but the consistent supply of nitrite to Anammox in the dilute mainstream remains a major bottleneck for wider applicability. Thus, an attractive alternative consists of combining Anammox bacteria with AOA, mimicking their successful partnership in the oligotrophic OMZ of the ocean. AOA has a remarkably high affinity for both oxygen (0.01 mg/L) and ammonium (0.001 mg/L)<sup>1,33</sup> and with such characteristics, AOA should thrive in the ammonia-deplete mainstream and replace AOB. In the case of encapsulated cells, it is essential to retain high AOA activity following gel immobilization. Although several approaches for crosslinking polyvinyl alcohol and SA have been used for the fabrication of hydrogel beads<sup>34–37</sup>, there is no information relevant to the immobilization of AOA.

As Anammox bacteria have been proven to grow in hydrogels previously our ultimate goal in this study was to demonstrate immobilization of active ammonia-oxidizing archaea in isolation in hydrogels formed by weak ionic interactions (calcium and barium) or physical interactions (modified PVA and sulfate). In addition to demonstrating retention of viable cells with gel entrapment, we conducted complementary analyses of stability and diffusivity of key nitrogen species (ammonium, nitrite, and nitrate) for different gel formulations to assist in the design of more active and robust

<sup>1</sup>Department of Civil and Environmental Engineering, University of Washington, Seattle, WA, USA. ✉email: [landreau.mat@gmail.com](mailto:landreau.mat@gmail.com)

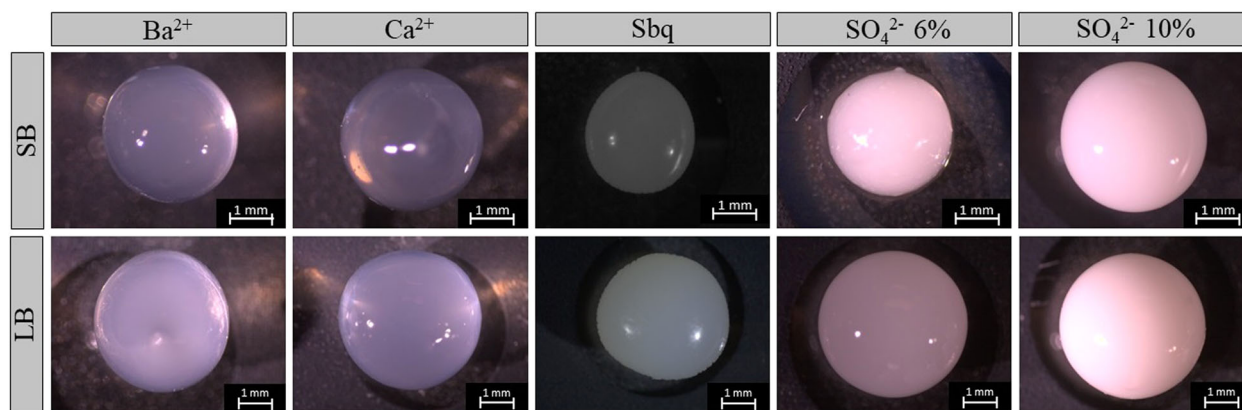


**Fig. 1 Morphology of hydrogel beads.** Macroscopic observations of small (SB) and large (LB) hydrogel beads cross-linked with barium ( $\text{Ba}^{2+}$ ), calcium ( $\text{Ca}^{2+}$ ), blue light (Sbq), and either sulfate 6% ( $\text{SO}_4^{2-}$  6%) or 10% ( $\text{SO}_4^{2-}$  10%).

**Table 1.** Average diameter of different hydrogel beads before and after 5 weeks of incubation.

	Small beads (SB)					Large beads (LB)				
	$\text{Ba}^{2+}$	$\text{Ca}^{2+}$	Sbq	$\text{SO}_4^{2-}$ 6%*	$\text{SO}_4^{2-}$ 10%	$\text{Ba}^{2+}$	$\text{Ca}^{2+}$	Sbq	$\text{SO}_4^{2-}$ 6%*	$\text{SO}_4^{2-}$ 10%
<i>Before</i>										
Mean ( $\mu\text{m}$ )	2449	2577	2739	3027	2847	4357	5471	4984	4399	4162
Std ( $\mu\text{m}$ )	155	85	198	207	144	138	174	152	102	290
Stat. group	a	a, b	a, b, c	c	b, c	a	b	c	a	a
<i>After</i>										
Mean ( $\mu\text{m}$ )	2359	2431	2765	3709	2873	4101	5281	4782	4491	4822
Std ( $\mu\text{m}$ )	149	87	257	182	197	138	149	500	121	326
Stat. group	a	a	c	b	c	a	b	b, c	c	c

Statistical groups differentiate types of hydrogels ( $\text{Ba}^{2+}$ ,  $\text{Ca}^{2+}$ , Sbq,  $\text{SO}_4^{2-}$  6%, and  $\text{SO}_4^{2-}$  10%) that have an average diameter significantly different for the same size (SB or LB) and incubation time (Before or After).

\*Correspond to conditions where incubation significantly affected beads' diameter.

hydrogel beads, and to provide practical information to help to select the appropriate formulation for future applications. We anticipate that this approach to bead fabrication, suitable for retaining a high activity of the slow-growing and fastidious AOA, will have general applications related to the study of AOA physiology in continuous flow systems and for advanced ammonium treatment of mainstream wastewater.

## RESULTS AND DISCUSSION

### Rheological behavior of different hydrogel beads in response to long-term incubation

The impact of polymerization on the size and shape of hydrogel carriers and cell viability can greatly influence the accessibility of microorganisms to nutrients and microbial growth within the polymer matrix<sup>38</sup>. To determine how the hydrogel composition may affect the characteristics of beads and the metabolic activity of AOA, we relied on different formulations of hydrogels previously used with AOB and Anammox bacteria along with activated sludge from wastewater<sup>39–41</sup>. Two of these formulations were based on weak ionic interactions (divalent ions), one used a combination of weak ionic interactions formed by calcium ions and physical bonding with photo click chemistry (PVA-stilbazolium), while the last one relied on the formation of physical sulfur bonds<sup>35,37,42,43</sup>. In order to evaluate differences in rheological behavior, we initially compared small (SB) and large (LB) PVA-SA beads (using 25 G needles and L/S 16 tubing, respectively) cross-

linked with the 4 selected agents: calcium (condition  $\text{Ca}^{2+}$ ), barium (condition  $\text{Ba}^{2+}$ ), sulfate (condition  $\text{SO}_4^{2-}$  6 and 10%) or blue light (condition Sbq) (Fig. 1). At 6% PVA, beads cross-linked with barium, calcium, and under blue light appeared round, smooth, and clear in color as previously described<sup>44,45</sup>. Beads cross-linked with sulfate (condition  $\text{SO}_4^{2-}$  6%) were white and softer in structure. The increase of PVA concentration up to 10% with sulfate (condition  $\text{SO}_4^{2-}$  10%) resulted in the formation of spherical beads similar to other conditions ( $\text{Ba}^{2+}$ ,  $\text{Ca}^{2+}$ , and Sbq) as already observed by Hashimoto and Furukawa<sup>13</sup>, and was therefore selected over  $\text{SO}_4^{2-}$  6% for the following experiments. After 5 weeks of incubation, no significant changes were observed regarding beads' morphology suggesting that beads structure remained unchanged over time.

To determine the impact of incubation on bead size over time, diameters were measured for all conditions before and after 5 weeks of incubation (Table 1). Before incubation, the average diameter of SB ranged from  $2449 \pm 155$  mm (condition  $\text{Ba}^{2+}$ ) to  $3027 \pm 207$  mm (condition  $\text{SO}_4^{2-}$  6%), while it varied between  $4162 \pm 290$  mm (condition  $\text{SO}_4^{2-}$  10%) and  $5471 \pm 174$  mm (condition  $\text{Ca}^{2+}$ ) with LB. For all conditions, intra-variability remained low (up to 7% with SB-Sbq) suggesting that a uniform sized population of beads was produced. Size uniformity ensures that bead diffusive behavior and entrained cellular activity will be consistent for the entire system<sup>46–49</sup>. Sulfate-cross-linked hydrogel formed the biggest SB (up to 24% compared to  $\text{Ba}^{2+}$ ), but the smallest LB (down to 16.5% compared to Sbq) due to the formation of a dense surface layer but a weaker and looser core by

boric acid that was more impactful in LB<sup>50</sup>. After 5 weeks of incubation, beads' diameter remained stable in most cases, varying between 0.93% for SB-Sbq and 5.69% for SB-Ca<sup>2+</sup>, with the exception of SB-SO<sub>4</sub><sup>2-</sup> 6% (+22.5%) and LB-SO<sub>4</sub><sup>2-</sup> 10% (+15.8%). The swelling of sulfate beads is attributed to the labile polar covalent interactions formed by boric acid, which give semi-solid properties to the hydrogel (even after treatment with sulfate) and contribute to the rubber-like elastic behavior of the beads<sup>51</sup>. While increased diameter can limit the diffusion of molecules to the bead core, leading to the formation of an inert zone, hydrogel swelling is also known to improve mass transfer rate<sup>52,53</sup>.

The increase of polymer concentration resulted in a significant increase of hydrogel viscosity, as previously observed by Oyanagi and Matsumoto<sup>54</sup>, and a decrease in droplet formation rate which was especially apparent for the production of SB. Although the boric acid method could therefore be challenging for large-scale applications, this limitation might be overcome either by producing beads in small consecutive batches or by increasing production rate using electrostatic, air-jet, or ultrasonic nozzle droplet generation techniques<sup>55–58</sup>. Another important factor for production is that using longer incubation times in boric acid to increase crosslinking and bead stability will also contribute to greater pH-related cell morbidity and associated decrease in microbial activity<sup>59</sup>. However, no inhibitory effect was observed in studies involving activated sludge, suggesting that this effect could be biomass-dependent<sup>60,61</sup>.

### Stability of different hydrogel beads to long-term incubation

The production of stable synthetic beads is essential for applications requiring long-term incubation in bioreactors. While PVA hydrogels have been used for extended periods of time in different environments (wastewater, soil, seawater, and industry)<sup>62–65</sup>, no study compared the stability of different cross-linked PVA-SA beads to determine the optimal hydrogel. In order to assess beads' resilience, the mass of polymer released in the liquid phase was measured after 5 weeks of incubation (Fig. 2). Among the conditions tested, two groups stood out clearly (1) beads cross-linked with barium (Ba<sup>2+</sup>), calcium (Ca<sup>2+</sup>), and light (Sbq), and (2) beads that were cross-linked with sulfate (SO<sub>4</sub><sup>2-</sup> 6 and 10%). In the former group, *ca* 1% (100 ± 10 mg) of the polymer was released in the liquid phase by SB and *ca* 1.7% (170 ± 35 mg) by LB. On the other hand, 0.2% (20 ± 1.5 mg) and 0.64% (63.7 ± 2.5 mg) of polymers were released by SB for SO<sub>4</sub><sup>2-</sup> 6 and 10% respectively, and *ca* 0.80% (80 ± 5 mg) with LB using the same conditions. While hydrogels remained stable with all formulations, polymers were

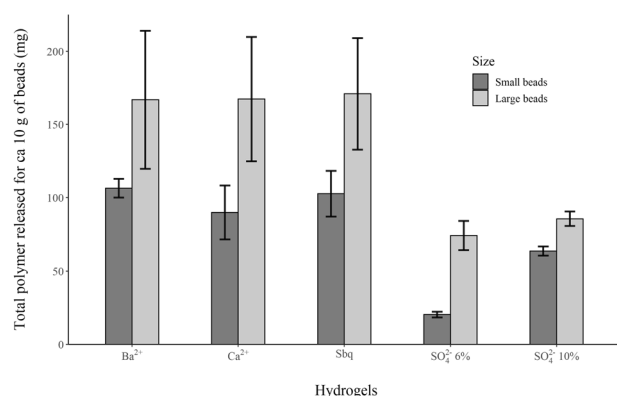


**Fig. 2 Mass of polymer released by hydrogel beads after incubation.** Concentration of polymer released in the liquid phase for small (Dark gray) and large beads (Light gray) cross-linked with barium (Ba<sup>2+</sup>), calcium (Ca<sup>2+</sup>), blue light (Sbq), and either sulfate 6% (SO<sub>4</sub><sup>2-</sup> 6%) or 10% (SO<sub>4</sub><sup>2-</sup> 10%) after 5 weeks of incubation. Error bars represent standard deviations.

detected in the liquid phase. Since PVA hydrogels have been reported to be stable at pH ranging from 6 to 8, it is most likely due to the presence of free polymers entrapped in the matrix during the immobilization process that leaked out progressively during incubation<sup>37</sup>. The significantly lower amount of polymer released (2–5 times) by sulfate-cross-linked hydrogels is likely due to the lower sensitivity of sulfate bonds to chelation by phosphate present in the medium compared to barium or calcium. In addition, sulfate bonds provide higher strength to the hydrogel that limits the leakage of polymers outside the beads<sup>51,66</sup>. It is also important to note that even though the sulfate-cross-linked hydrogels benefited from a higher cross-linker concentration (51 mM vs. 36 mM) during the polymerization process compared to other conditions, it was reported that for cross-linker concentrations within the same range (9–22 mM) no significant effect was observed on the gel strength of PVA hydrogels<sup>67</sup>. The significant difference of leakage observed between SB and LB, ranging from 26% for SO<sub>4</sub><sup>2-</sup> 10 to 73% for SO<sub>4</sub><sup>2-</sup> 6% (with an average around 45%), also reflects the importance to examine exposure time (and herewith associated diffusion time) of cross-linkers into different bead sizes to allow a complete and stable polymerization<sup>46,47,49</sup>. Finally, the variability between replicates was much lower (around 80%) with sulfate-bound beads than with other conditions, suggesting that polymerization was more uniform with sulfate.

Overall, sulfate-cross-linked hydrogel beads maintained a better physical and mechanical stability (surface, size, and matrix) after a long-term incubation in comparison to calcium-, barium-, or light-linked beads.

### Diffusion behavior of nitrogen species in different hydrogels

Mass transfer mechanisms dictate the supply of nutrients and metabolites in and out of the hydrogel and are therefore crucial to overall reaction rates<sup>68</sup>. As diffusion will greatly affect microbial growth, a better understanding of the physical properties of synthetic beads can help select hydrogels adapted to specific substrates, and therefore greatly improve the activities of targeted species following gel immobilization. Here we examined the diffusion coefficients of substrate and metabolites of greatest relevance to nitrifiers (ammonium, nitrite, and nitrate) for 4 different hydrogels (Ba<sup>2+</sup>, Ca<sup>2+</sup>, Sbq, and SO<sub>4</sub><sup>2-</sup> 10%) in the two-compartment setup (Fig. 3), while the sulfate-cross-linked hydrogels were too squishy for diffusion tests at 6% PVA. The diffusion coefficient of ammonium was the highest among the three nitrogen species ranging from  $2.17 \times 10^{-9} \pm 4 \times 10^{-10}$  m<sup>2</sup>/s (condition SO<sub>4</sub><sup>2-</sup> 10%) to  $3.04 \times 10^{-9} \pm 3 \times 10^{-10}$  m<sup>2</sup>/s (condition

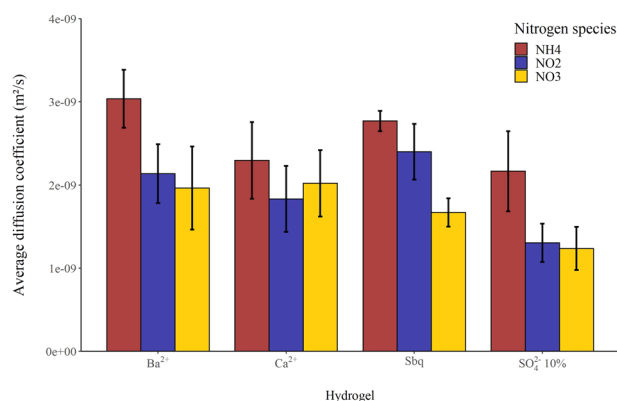


**Fig. 3 Diffusion of nitrogen species in hydrogels.** Diffusion coefficients of ammonium (Red), nitrite (Blue), and nitrate (Yellow) in a PVA-SA hydrogel cross-linked with barium (Ba<sup>2+</sup>), calcium (Ca<sup>2+</sup>), light (Sbq), or sulfate (SO<sub>4</sub><sup>2-</sup> 10%). Error bars represent standard deviations.

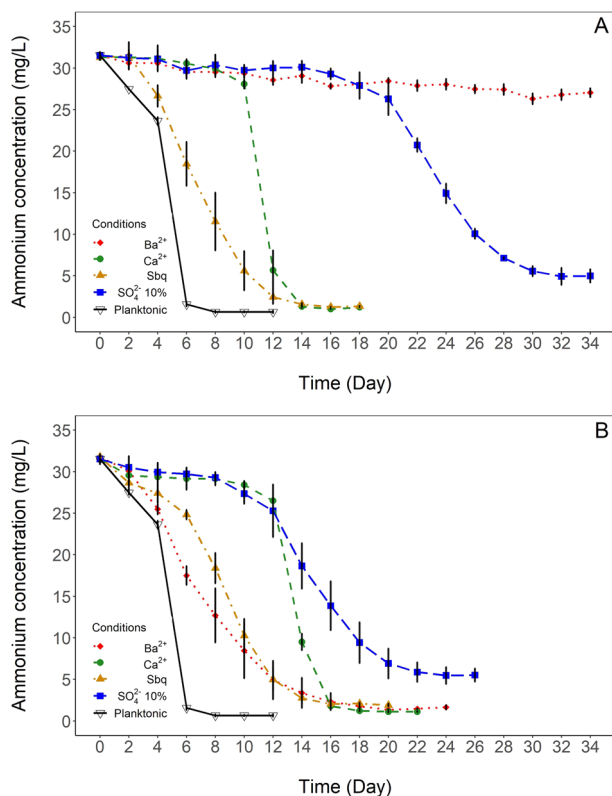


**Fig. 4 Ammonium removal by immobilized AOA.** Ammonium consumption over time by planktonic vs. entrapped AOA in small (**A**) and large beads (**B**) cross-linked with barium (Ba<sup>2+</sup>), calcium (Ca<sup>2+</sup>), light (Sbq), or sulfate (SO<sub>4</sub><sup>2-</sup> 10%). Error bars represent standard deviations.

Ba<sup>2+</sup>). In contrast, diffusion coefficients ranged between  $1.31 \times 10^{-9} \pm 2 \times 10^{-10} \text{ m}^2/\text{s}$  (condition SO<sub>4</sub><sup>2-</sup> 10%) and  $2.40 \times 10^{-9} \pm 3 \times 10^{-10} \text{ m}^2/\text{s}$  (condition Sbq) for nitrite, and between  $1.24 \times 10^{-9} \pm 2 \times 10^{-10} \text{ m}^2/\text{s}$  (condition SO<sub>4</sub><sup>2-</sup> 10%) and  $2.02 \times 10^{-9} \pm 3 \times 10^{-10} \text{ m}^2/\text{s}$  (condition Ca<sup>2+</sup>) for nitrate. These coefficients were similar to the ones measured by Ali et al.<sup>69</sup> with immobilized biomass (2.899, 2.796, and  $2.782 \times 10^{-9} \text{ m}^2/\text{s}$  for NH<sub>4</sub><sup>+</sup>, NO<sub>2</sub><sup>-</sup>, NO<sub>3</sub><sup>-</sup>, respectively) in PVA-SA beads cross-linked with calcium, and up to 4 times higher (for condition Ba<sup>2+</sup>) than the coefficients measured with granular biomass at 37 °C (0.861, 0.831, and  $0.826 \times 10^{-9} \text{ m}^2/\text{s}$  for NH<sub>4</sub><sup>+</sup>, NO<sub>2</sub><sup>-</sup>, NO<sub>3</sub><sup>-</sup>, respectively).

These results confirmed that hydrogels provide better mass transfer of nitrogen species than natural granules. The comparison of ammonium and nitrite/nitrate diffusion coefficients also highlighted a significant difference between positively and negatively charged nitrogen species (ammonium coefficient being 30–40% higher), particularly visible with a barium- and sulfate-cross-linked hydrogels. This could be explained by increased interactions between the hydrogel residues and nitrogen species at a very low ionic solution strength (*ca* 1 mmol/L) that may be the consequence of an incomplete screening of the binding sites that affected the progression of solutes throughout the matrix<sup>70,71</sup>. Therefore, if more carboxyl groups from alginate remained available with barium and sulfate compared to calcium formulations, these anionic functional groups could have limited the diffusion of nitrite and nitrate through the polymeric network. These diffusive characteristics are of direct relevance to a treatment technology using co-immobilization of AOA and Anammox bacteria in hydrogels. A longer retention time of nitrite generated by the AOA could facilitate the removal of ammonium

by Anammox bacteria as long as nitrate concentration remains low (<100 mg/L) in the hydrogel<sup>72</sup>.

Finally, lower diffusion coefficients were observed with sulfate hydrogels in comparison to other hydrogels, up to *ca.* 35% compared to barium. Considering that all three nitrogen species were similarly affected, it is reasonable to conclude that the reduction of mass transfer can be attributed to the increased PVA concentration (10% instead of 6%) in the hydrogel<sup>73</sup>. Due to the softness of the sulfate-bound hydrogel at 6% PVA, it was not possible to confirm this hypothesis. The higher diffusivity of substrates into gel beads compared to natural granular sludge systems<sup>74,75</sup> will influence the optimal bead size and reactor conditions (DO concentrations) required for optimal process performance.

### Ammonium oxidation by immobilized AOA

Retention of ammonia oxidation activity using alternative methods of hydrogel fabrication was evaluated by entrapping a strain of AOA. The use of this sensitive and slow-growing ammonia oxidizer served to evaluate gel fabrication conditions that retain highly active biomass (Fig. 4). In small beads, the lag phase in activity was shortest for the PVA-Sbq hydrogels, where initial ammonium oxidation was observed after 2 days, with an approximate consumption of 3.0 mg NH<sub>4</sub><sup>+</sup>-N/d and a complete consumption on day 14. In contrast, ammonium was only consumed after 10 and 16 days for conditions Ca<sup>2+</sup> and SO<sub>4</sub><sup>2-</sup> 10%, respectively, at an average rate of 6.8 mg and 1.7 mg NH<sub>4</sub><sup>+</sup>-N/d (over the next 4 and 18 days, respectively). No significant ammonium removal was observed in the barium-cross-linked hydrogel. In LB, no lag phase was observed for conditions Ba<sup>2+</sup> and Sbq, and approximately 2.5 mg NH<sub>4</sub><sup>+</sup>-N/d was removed over 20 days for both conditions. On the other hand, ammonium oxidation was only detected after 10 days for conditions Ca<sup>2+</sup> and SO<sub>4</sub><sup>2-</sup> 10%, where it reached an average rate of 4.0 mg and 1.86 mg NH<sub>4</sub><sup>+</sup>-N/d over the next 8 and 16 days, respectively.

No trend was observed for all four conditions regarding the effect of bead diameter on the duration of the lag phase of ammonium consumption rate suggesting that bead size did not significantly impact the removal efficiency as previously observed by Sun et al.<sup>20</sup> with entrapped nitrifying bacteria, possibly indicating that active cells were mostly located close from the surface. The sulfate-bound hydrogel is an exception, as SB displayed a much longer lag phase, attributed to the cellular stress caused by the boric acid soaking step, while LB provided a protective core farther removed from the high boric acid environment<sup>76</sup>. A similar pattern was observed for the barium-cross-linked hydrogel beads, where locally high barium concentration in the hydrogel of SB inhibited AOA activity<sup>77</sup>. As for conditions using calcium, cells entrapped in hydrogels containing PVA-Sbq displayed a much shorter lag phase than without PVA-Sbq (day 0 and 2 vs. day 10), highlighting an inhibitory effect of this polymer composition on AOA. While the addition of polyethylene glycol to PVA-Sbq has been shown to enhance enzymatic activity by facilitating the diffusion of substrates<sup>78</sup>, we demonstrated no significant difference in diffusion in the present study. We, therefore, hypothesize that the addition of positively charged PVA-Sbq might have counter-balanced the negative charges of PVA, which facilitated the release of excess calcium and reduced its inhibitory effect. In comparison to embedded AOA, ammonium was completely oxidized within the first 6 days (rate = 5 mg/L/d) with planktonic cells. The difference observed between free-cell and entrapped AOA is a reflection of both the initial stress of the polymerization process<sup>79–81</sup> and reduced substrate mass transfer of ammonium in the hydrogel<sup>82</sup>. The reduction of carbon source uptake, bicarbonate in the present study, due to the diffusion limitation might also have played a role in the slower metabolic activity. However, it is notable that

following adaptation, the small beads cross-linked with  $\text{Ca}^{2+}$  exhibited rates of ammonia removal comparable to the planktonic cells. This suggests that a hydrogel bead technology could be used to retain high ammonia-oxidizing activity by AOA in a full-scale water treatment application or for research purposes.

### Perspectives

The use of calcium- or sulfate-cross-linked hydrogel beads for non-biofilm forming (AOA) strains is a promising approach for potential long-term applications in microbial ecology and biotechnological application. As an example, the immobilization of AOA in hydrogels opens new opportunities for future applications where retention of viable AOA biomass is critical and unachievable with planktonic cells such as for the effluent polishing of ammonia-depleted mainstream wastewater. Nonetheless, we anticipate that further development of entrapment protocols could enhance removal efficiency and render it more attractive for large-scale applications. A key objective will be to meet volume requirements associated with treatment plant applications. Therefore, future studies should work on the development of embedding procedures adapted to the industrial-scale production of hydrogel beads in a timely manner while maintaining high metabolic activity. In addition, a special focus should be made on the improvement of ammonium conversion rate to optimize production and operating costs, and performances in ammonium-depleted wastewater (mainstream wastewater) should be investigated for comparison with existing approaches. Two complementary strategies can already emerge from the current study: increase the surface to volume ratio (i.e., decrease beads' diameter), and increase cell density in hydrogel beads. Finally, the combination of Anammox bacteria to AOA should also be explored to perform a complete ammonium removal and decrease space requirements as it already exists with AOB<sup>83</sup>.

## METHODS

### AOA culture medium

The AOA culture medium used in the present study was composed of (per liter): 0.147 g  $\text{CaCl}_2 \cdot 2\text{H}_2\text{O}$ , 0.049 g  $\text{MgSO}_4 \cdot 7\text{H}_2\text{O}$ , 0.075 g KCl, 0.585 g NaCl, 1.192 g HEPES (4-(2-hydroxyethyl)-1-piperazineethanesulfonic acid), 16.8 mg  $\text{NaHCO}_3$ , 2.753 mg FeNa-EDTA (Ethylenediaminetetraacetic acid ferric sodium salt), 2.18 mg  $\text{K}_2\text{HPO}_4$ , and 30 mg  $\text{NH}_4\text{Cl}$ . After autoclaving (121 °C for 20 min), 1 ml of sterile trace elements solution was added to the medium. The composition of the trace elements solution was (per liter): 190 mg  $\text{CoCl}_2 \cdot 6\text{H}_2\text{O}$ , 144 mg  $\text{ZnSO}_4 \cdot 7\text{H}_2\text{O}$ , 100 mg  $\text{MnCl}_2 \cdot 4\text{H}_2\text{O}$ , 36 mg  $\text{NaMoO}_4 \cdot 2\text{H}_2\text{O}$ , 30 mg  $\text{H}_3\text{BO}_3$ , 24 mg  $\text{NiCl}_2 \cdot 6\text{H}_2\text{O}$ , 2 mg  $\text{CuCl}_2 \cdot 2\text{H}_2\text{O}$ . The pH was set at 7.6.

### Stability tests

Three different types of polymers were used to prepare hydrogel beads: PVA, Polyvinyl alcohol N-methyl-4(4'-formylstyryl)pyridinium methosulfate acetal (PVA-stilbazolium or PVA-Sbq), and SA (Sigma Aldrich (St-Louis, USA) and Polysciences Inc. (Warrington, USA)).

Hydrogel stability was assessed for 5 different types of beads produced as follows: 6% PVA—2% SA cross-linked with 4%  $\text{CaCl}_2$  (condition  $\text{Ca}^{2+}$ ), 6% PVA—2% SA cross-linked with 4%  $\text{BaCl}_2$  (condition  $\text{Ba}^{2+}$ ), 3% PVA—3% PVA-Sbq—2% SA cross-linked with 4%  $\text{CaCl}_2$  under blue light 465 nm (condition Sbq), 6 or 10% PVA—2% SA cross-linked with 4%  $\text{CaCl}_2$  in saturated boric acid followed by 7.3%  $\text{NaSO}_4$  (condition  $\text{SO}_4^{2-}$  6 and 10%, respectively). All polymer concentrations are given as final concentrations.

Beads were prepared by extruding the polymer mixture via a peristaltic pump through a 25 G needle or a 16L/S tubing into a cross-linking solution to form small and large beads of approximately 2.5 and 4.7 mm, respectively. After an hour of incubation, beads were collected on a 1.4-mm sieve and washed with a 0.9% NaCl solution. For each condition, three 100-ml serum bottles (VWR, Radnor, USA) containing 10 ml of beads and 40 ml of AOA culture medium were incubated horizontally at 30 °C under agitation (90 rpm) for 5 weeks.

To assess hydrogel stability, general aspect and bead size distribution were measured before and after incubation using a stereoscope Stemi 508 (Zeiss, Oberkochen, Germany). In addition, polymer release was quantified after the 5-week incubation by drying 20 ml of the supernatant at 65 °C and weighting the total carbon and mineral content followed by carbonization in a muffle furnace (Thermo Scientific) at 500 °C to measure the mineral content only. The mass of mineral content was then subtracted from total content values in order to obtain the amount of polymer released. A control serum bottle without beads was incubated and quantified using the same protocol.

### Diffusion test

The diffusion coefficients of ammonium, nitrite, and nitrate for different hydrogels (condition  $\text{Ba}^{2+}$ ,  $\text{Ca}^{2+}$ ,  $\text{SO}_4^{2-}$  10%, and Sbq) were characterized by measuring their transfer rate through a hydrogel membrane in a two-compartment model (Fig. 5). Disks of hydrogels (diameter: 25 mm, thickness: 10 mm) were cast into a circular mold, squeezed between 2 metal filter disks to prevent swelling, and incubated for 2 h in their respective crosslinking solution. The assemblies (hydrogel disc + mold) were then washed with DI water to remove the excess of the cross-linking solution, placed between 2 glass compartments (volume = 32 ml) containing DI water or a solution of nitrogen species (15 mg N/L), and maintained at 20 °C. Concentrations of nitrogen species in both compartments were measured spectrophotometrically (Gallery™ Fisher Scientific, Hampton, USA) at time 0 and after 8, 24, 48, 72, and 96 h. All experiments were run in duplicate. The average diffusion coefficient was calculated following Fick's first law of diffusion:

$$D = \frac{J \cdot dX}{dC}$$

where  $D$  is the diffusion coefficient or diffusivity ( $\text{m}^2 \text{s}^{-1}$ ),  $J$  is the diffusion flux ( $\text{mol m}^{-2} \text{s}^{-1}$ ),  $dC$  is the difference of concentrations between the two compartments ( $\text{mol/m}^3$ ) and  $dX$  is the hydrogel thickness ( $m$ ).

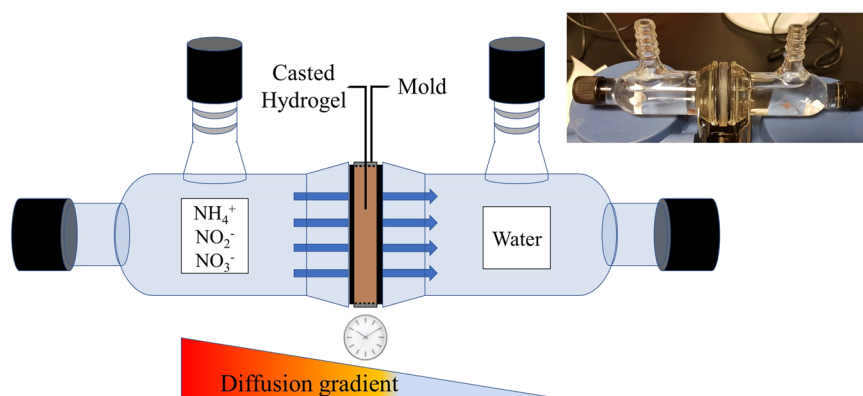


**Fig. 5** Two-compartment setup for the measurement of diffusion rate in hydrogels. A disc of hydrogel is placed between two glass tanks containing a solution of ammonium, nitrite or nitrate, and deionized water respectively.

The diffusive flux  $J$  was determined from the difference of concentrations measured in the receiving tank between two-time points (excluding  $T_0$ ) as follows:

$$J = \frac{(M_n + 1 - M_n) \cdot V}{dT \cdot S}$$

where  $M_n$  and  $M_{n+1}$  is the molar concentration ( $\text{mol L}^{-1}$ ) in the receiving tank at  $t_n$  and  $t_{n+1}$  respectively,  $V$  is the volume of the tank (L),  $dT$  is the time between  $t_n$  and  $t_{n+1}$  (s) and  $S$  is the surface area of the hydrogel ( $\text{m}^2$ ).

### AOA biomass

A strain of AOA (DW1) earlier enriched by the Bollman laboratory from Lake Delaware, Ohio sediments were used to inoculate 50 ml of mineral salt medium (30 mg/L  $\text{N-NH}_4^+$ ). The enrichment was prepared by incubating the sample at 25 °C until 80% of ammonium was consumed and then filtered (0.45  $\mu\text{m}$ ) to specifically enrich small cells such as AOA<sup>84</sup>. Every 2–4 weeks, 50 ml of DW1 enrichment culture was used to inoculate 450 ml of AOA medium in order to maintain the activity of cells. Prior to cell immobilization, 2 l of AOA culture medium was inoculated with 100 ml of DW1 enrichment and incubated at 30 °C. After complete consumption of ammonium, the culture was filtered on a Büchner funnel using GTTP filter 0.2  $\mu\text{m}$  (Millipore), cells were resuspended in 100 ml of sterile AOA culture medium and used within 24 h for the experiments.

### Cell immobilization and culture test

Approximately one hundred milliliters of hydrogel beads were produced by mixing 10 ml of AOA suspension ( $\text{ca } 10^8$  cells/ml) with 90 ml of autoclaved polymers solution following the crosslinking conditions described in section “Stability of different hydrogel beads to long-term incubation” ( $\text{Ca}^{2+}$ ,  $\text{Ba}^{2+}$ ,  $\text{SO}_4^{2-}$  10%, and  $\text{Sbq}$ ). Activity for each condition was determined in triplicate by incubating 10 ml of wet beads in a 100-ml serum bottle containing 30 ml of AOA culture medium. As a control, 1 ml of the AOA suspension was used to inoculate three serum bottles containing 30 ml of AOA medium. Serum bottles were incubated aerobically at 30 °C under agitation (150 rpm). Every 2 days, ammonium concentration in the supernatant was measured using Gallery™ Plus Discrete Analyzer (Thermo Fisher Scientific, USA).

### DATA AVAILABILITY

The data that support the findings of this study are available from the corresponding author upon reasonable request.

Received: 18 January 2021; Accepted: 2 August 2021;

Published online: 09 September 2021

### REFERENCES

- Park, H. D., Wells, G. F., Bae, H., Criddle, C. S. & Francis, C. A. Occurrence of ammonia-oxidizing archaea in wastewater treatment plant bioreactors. *Appl. Environ. Microbiol.* **72**, 5643–5647 (2006).
- Zhang, T. et al. Occurrence of ammonia-oxidizing Archaea in activated sludges of a laboratory scale reactor and two wastewater treatment plants. *J. Appl. Microbiol.* **107**, 970–977 (2009).
- Stahl, D. A. & de la Torre, J. R. Physiology and diversity of ammonia-oxidizing archaea. *Annu. Rev. Microbiol.* **66**, 83–101 (2012).
- de la Torre, J. R., Walker, C. B., Ingalls, A. E., Konneke, M. & Stahl, D. A. Cultivation of a thermophilic ammonia oxidizing archaeon synthesizing crenarchaeol. *Environ. Microbiol.* **10**, 810–818 (2008).
- Lehtovirta-Morley, L. E., Stoecker, K., Vilcinskas, A., Prosser, J. I. & Nicol, G. W. Cultivation of an obligate acidophilic ammonia oxidizer from a nitrifying acid soil. *Proc. Natl Acad. Sci. USA* **108**, 15892–15897 (2011).
- Konneke, M. et al. Isolation of an autotrophic ammonia-oxidizing marine archaeon. *Nature* **437**, 543–546 (2005).
- Schleper, C. & Nicol, G. W. Ammonia-oxidizing archaea—physiology, ecology and evolution. *Adv. Microb. Physiol.* **57**, 1–41 (2010).
- Bollmann, A., French, E. & Laanbroek, H. J. Isolation, cultivation, and characterization of ammonia-oxidizing bacteria and archaea adapted to low ammonium concentrations. *Methods Enzymol.* **486**, 55–88 (2011).
- Cassidy, M., Lee, H. & Trevors, J. Environmental applications of immobilized microbial cells: a review. *J. Ind. Microbiol.* **16**, 79–101 (1996).
- Hennink, W. E. & van Nostrum, C. F. Novel crosslinking methods to design hydrogels. *Adv. Drug Deliv. Rev.* **64**, 223–236 (2012).
- Rathore, S., Desai, P. M., Liew, C. V., Chan, L. W. & Heng, P. W. S. Micro-encapsulation of microbial cells. *J. Food Eng.* **116**, 369–381 (2013).
- Cinquin, C., Le Blay, G., Fliss, I. & Lacroix, C. Immobilization of infant fecal microbiota and utilization in an in vitro colonic fermentation model. *Microb. Ecol.* **48**, 128–138 (2004).
- Hashimoto, S. & Furukawa, K. Immobilization of activated sludge by PVA-boric acid method. *Biotechnol. Bioeng.* **30**, 52–59 (1987).
- Landreau, M. et al. Entrapment of anaerobic thermophilic and hyperthermophilic marine micro-organisms in a gellan/xanthan matrix. *J. Appl. Microbiol.* **120**, 1531–1541 (2016).
- Sumino, T., Nakamura, H., Mori, N., Kawaguchi, Y. & Tada, M. Immobilization of nitrifying bacteria in porous pellets of urethane gel for removal of ammonium nitrogen from waste-water. *Appl. Microbiol. Biotechnol.* **36**, 556–560 (1992).
- Li, Z., Zhang, Z., Li, J. & Zhang, Z. Comparative study of the nitrification characteristics of two different nitrifier immobilization methods. *Biodegradation* **20**, 859–865 (2009).
- Isaka, K., Kimura, Y., Yamamoto, T., Osaka, T. & Tsuneda, S. Complete autotrophic denitrification in a single reactor using nitritation and anammox gel carriers. *Bioresour. Technol.* **147**, 96–101 (2013).
- Sakairi, M. A. C., Yasuda, K. & Matsumura, M. Nitrogen removal in seawater using nitrifying and denitrifying bacteria immobilized in porous cellulose carrier. *Water Sci. Technol.* **34**, 267–274 (1996).
- Bai, X., Ye, Z.-f., Li, Y.-f., Zhou, L.-C. & Yang, L.-Q. Preparation of crosslinked macroporous PVA foam carrier for immobilization of microorganisms. *Process Biochem.* **45**, 60–66 (2010).
- Sun, J., Liu, J., Liu, Y., Li, Z. & Nan, J. Optimization of entrapping conditions of nitrifying bacteria and selection of entrapping agent. *Procedia Environ. Sci.* **8**, 166–172 (2011).
- Qiao, S., Tian, T., Duan, X., Zhou, J. & Cheng, Y. Novel single-stage autotrophic nitrogen removal via co-immobilizing partial nitrifying and anammox biomass. *Chem. Eng. J.* **230**, 19–26 (2013).
- Rongsayamanont, C., Limpiyakorn, T. & Khan, E. Effects of inoculum type and bulk dissolved oxygen concentration on achieving partial nitrification by entrapped-cell-based reactors. *Bioresour. Technol.* **164**, 254–263 (2014).
- Bae, H., Choi, M., Chung, Y.-C., Lee, S. & Yoo, Y. J. Core-shell structured poly (vinyl alcohol)/sodium alginate bead for single-stage autotrophic nitrogen removal. *Chem. Eng. J.* **322**, 408–416 (2017).
- Dong, Y., Zhang, Y. & Tu, B. Immobilization of ammonia-oxidizing bacteria by polyvinyl alcohol and sodium alginate. *Braz. J. Microbiol.* **48**, 515–521 (2017).
- Hui, B., Zhang, Y. & Ye, L. Preparation of PVA hydrogel beads and adsorption mechanism for advanced phosphate removal. *Chem. Eng. J.* **235**, 207–214 (2014).
- Lee, K. Y. & Mooney, D. J. Alginate: properties and biomedical applications. *Prog. Polym. Sci.* **37**, 106–126 (2012).
- Yan, J., Jettten, M., Rang, J. & Hu, Y. Comparison of the effects of different salts on aerobic ammonia oxidizers for treating ammonium-rich organic wastewater by free and sodium alginate immobilized biomass system. *Chemosphere* **81**, 669–673 (2010).
- Hill, C. B. & Khan, E. A comparative study of immobilized nitrifying and co-immobilized nitrifying and denitrifying bacteria for ammonia removal from sludge digester supernatant. *Water Air Soil Pollut.* **195**, 23 (2008).
- Xiangli, Q., Zhe, L., Zhiwei, L., Yinglin, Z. & Zhongjia, Z. Immobilization of activated sludge in poly (ethylene glycol) by UV technology and its application in micro-polluted wastewater. *Biochem. Eng. J.* **50**, 71–76 (2010).
- Bae, H. et al. Optimization of the mechanical strength of PVA/alginate gel beads and their effects on the ammonia-oxidizing activity. *Desalination Water Treat.* **53**, 2412–2420 (2015).
- Isaka, K., Kimura, Y., Matsuura, M., Osaka, T. & Tsuneda, S. First full-scale nitritation-anammox plant using gel entrapment technology for ammonia plant effluent. *Biochem. Eng. J.* **122**, 115–122 (2017).
- Siegrist, H., Salzgeber, D., Eugster, J. & Joss, A. Anammox brings WWTP closer to energy autarky due to increased biogas production and reduced aeration energy for N-removal. *Water Sci. Technol.* **57**, 383–388 (2008).
- Martens-Habbena, W., Berube, P. M., Urakawa, H., de la Torre, J. R. & Stahl, D. A. Ammonia oxidation kinetics determine niche separation of nitrifying Archaea and Bacteria. *Nature* **461**, 976–979 (2009).
- Wu, K. Y. & Wisecarver, K. D. Cell immobilization using PVA crosslinked with boric acid. *Biotechnol. Bioeng.* **39**, 447–449 (1992).
- Hertzberg, S., Moen, E., Vogelsang, C. & Østgaard, K. Mixed photo-cross-linked polyvinyl alcohol and calcium-alginate gels for cell entrapment. *Appl. Microbiol. Biotechnol.* **43**, 10–17 (1995).
- Zhang, L. S., Wu, W. Z. & Wang, J. L. Immobilization of activated sludge using improved polyvinyl alcohol (PVA) gel. *J. Environ. Sci.* **19**, 1293–1297 (2007).

37. Takei, T., Ikeda, K., Ijima, H. & Kawakami, K. Fabrication of poly (vinyl alcohol) hydrogel beads crosslinked using sodium sulfate for microorganism immobilization. *Process Biochem.* **46**, 566–571 (2011).
38. Jen, A. C., Wake, M. C. & Mikos, A. G. Review: Hydrogels for cell immobilization. *Biotechnol. Bioeng.* **50**, 357–364 (1996).
39. Vogelsang, C., Husby, A. & Østgaard, K. Functional stability of temperature-compensated nitrification in domestic wastewater treatment obtained with PVA-SbQ/alginate gel entrapment. *Water Res.* **31**, 1659–1664 (1997).
40. Ali, M., Oshiki, M. & Okabe, S. Simple, rapid and effective preservation and reactivation of anaerobic ammonium oxidizing bacterium "Candidatus Brocadia sinica". *Water Res.* **57**, 215–222 (2014).
41. Xu, X. et al. Nitrogen removal and microbial diversity of activated sludge entrapped in modified poly (vinyl alcohol)–sodium alginate gel. *Int. Biodeterior. Biodegrad.* **125**, 243–250 (2017).
42. Smidsrød, O. & Skjå, G. Alginate as immobilization matrix for cells. *Trends Biotechnol.* **8**, 71–78 (1990).
43. Ichimura, K. A convenient photochemical method to immobilize enzymes. *J. Polym. Sci. Polym. Chem. Ed.* **22**, 2817–2828 (1984).
44. Quan, L. M., Khanh do, P., Hira, D., Fujii, T. & Furukawa, K. Reject water treatment by improvement of whole cell anammox entrapment using polyvinyl alcohol/alginate gel. *Biodegradation* **22**, 1155–1167 (2011).
45. Vogelsang, C., Schramm, A., Picioroanu, C., Van Loosdrecht, M. C. & Østgaard, K. Microbial community analysis by FISH for mathematical modelling of selective enrichment of gel-entrapped nitrifiers obtained from domestic wastewater. *Hydrobiologia* **469**, 165–178 (2002).
46. Chung, T.-P., Tseng, H.-Y. & Juang, R.-S. Mass transfer effect and intermediate detection for phenol degradation in immobilized *Pseudomonas putida* systems. *Process Biochem.* **38**, 1497–1507 (2003).
47. Chen, K.-C., Lin, Y.-H., Chen, W.-H. & Liu, Y.-C. Degradation of phenol by PAA-immobilized *Candida tropicalis*. *Enzym. Microb. Technol.* **31**, 490–497 (2002).
48. Barranco-Florido, E., García-Garibay, M., Gomez-Ruiz, L. & Azaola, A. Immobilization system of *Kluyveromyces marxianus* cells in barium alginate for inulin hydrolysis. *Process Biochem.* **37**, 513–519 (2001).
49. Speirs, E. D., Halling, P. & McNeil, B. The importance of bead size measurement in mass-transfer modelling with immobilised cells. *Appl. Microbiol. Biotechnol.* **43**, 440–444 (1995).
50. Zhang, Y., Hui, B. & Ye, L. Reactive toughening of polyvinyl alcohol hydrogel and its wastewater treatment performance by immobilization of microorganisms. *RSC Adv.* **5**, 91414–91422 (2015).
51. Idris, A., Zain, N. A. M. & Suhaimi, M. S. Immobilization of Baker's yeast invertase in PVA–alginate matrix using innovative immobilization technique. *Process Biochem.* **43**, 331–338 (2008).
52. Lewinska, D., Rosinski, S. & Werynski, A. Influence of process conditions during impulsed electrostatic droplet formation on size distribution of hydrogel beads. *Artif. Cells Blood Substit. Immobil. Biotechnol.* **32**, 41–53 (2004).
53. Kim, S. W., Bae, Y. H. & Okano, T. Hydrogels: swelling, drug loading, and release. *Pharm. Res.* **9**, 283–290 (1992).
54. Ōyanagi, Y. & Matsumoto, M. Viscosity of moderately concentrated aqueous solutions of polyvinyl alcohol. *J. Colloid Sci.* **17**, 426–438 (1962).
55. Bugarski, B. et al. Electrostatic droplet generation: mechanism of polymer droplet formation. *AIChE J.* **40**, 1026–1031 (1994).
56. Bugarski, B. M., Obradovic, B., Nedovic, V. A. & Poncelet, D. in *Fundamentals Of Cell Immobilisation Biotechnology*. 277–294 (Springer, Berlin, Germany, 2004).
57. Goosen, M. F., O'Shea, G. M., Gharapetian, H. M., Chou, S. & Sun, A. M. Optimization of microencapsulation parameters: semipermeable microcapsules as a bioartificial pancreas. *Biotechnol. Bioeng.* **27**, 146–150 (1985).
58. Stormo, K. E. & Crawford, R. L. Preparation of encapsulated microbial cells for environmental applications. *Appl. Environ. Microbiol.* **58**, 727–730 (1992).
59. Lozinsky, V. & Plieva, F. Poly (vinyl alcohol) cryogels employed as matrices for cell immobilization. 3. Overview of recent research and developments. *Enzym. Microb. Technol.* **23**, 227–242 (1998).
60. Shammass, N. K. Interactions of temperature, pH, and biomass on the nitrification process. *J. Water Pollut. Control Fed.* **58**, 52–59 (1986).
61. Painter, H. & Lovelless, J. Effect of temperature and pH value on the growth-rate constants of nitrifying bacteria in the activated-sludge process. *Water Res.* **17**, 237–248 (1983).
62. Cao, G.-M., Zhao, Q.-X., Sun, X.-B. & Zhang, T. Characterization of nitrifying and denitrifying bacteria coimmobilized in PVA and kinetics model of biological nitrogen removal by coimmobilized cells. *Enzym. Microb. Technol.* **30**, 49–55 (2002).
63. Cunningham, C., Ivshina, I., Lozinsky, V., Kuyukina, M. & Philp, J. Bioremediation of diesel-contaminated soil by microorganisms immobilised in polyvinyl alcohol. *Int. Biodeterior. Biodegrad.* **54**, 167–174 (2004).
64. Furukawa, K., Ike, A., Ryu, S.-L. & Fujita, M. Nitrification of NH<sub>4</sub>-N polluted sea water by immobilized acclimated marine nitrifying sludge (AMNS). *J. Ferment. Bioeng.* **76**, 515–520 (1993).
65. Verbelen, P. J., De Schutter, D. P., Delvaux, F., Verstrepen, K. J. & Delvaux, F. R. Immobilized yeast cell systems for continuous fermentation applications. *Biotechnol. Lett.* **28**, 1515–1525 (2006).
66. Zain, N. A. M., Suhaimi, M. S. & Idris, A. Development and modification of PVA–alginate as a suitable immobilization matrix. *Process Biochem.* **46**, 2122–2129 (2011).
67. Kjøniksen, A.-L. & Nyström, B. Effects of polymer concentration and cross-linking density on rheology of chemically cross-linked poly (vinyl alcohol) near the gelation threshold. *Macromolecules* **29**, 5215–5222 (1996).
68. Karel, S. F., Libicki, S. B. & Robertson, C. R. The immobilization of whole cells: engineering principles. *Chem. Eng. Sci.* **40**, 1321–1354 (1985).
69. Ali, M. et al. Rapid and successful start-up of anammox process by immobilizing the minimal quantity of biomass in PVA-SA gel beads. *Water Res.* **79**, 147–157 (2015).
70. Peters, A. J., Zhang, H. & Davison, W. Performance of the diffusive gradients in thin films technique for measurement of trace metals in low ionic strength freshwaters. *Anal. Chim. Acta* **478**, 237–244 (2003).
71. Fatin-Rouge, N., Milon, A., Buffle, J., Goulet, R. R. & Tessier, A. Diffusion and partitioning of solutes in agarose hydrogels: the relative influence of electrostatic and specific interactions. *J. Phys. Chem. B* **107**, 12126–12137 (2003).
72. Strous, M., Kuenen, J. G. & Jetten, M. S. Key physiology of anaerobic ammonium oxidation. *Appl. Environ. Microbiol.* **65**, 3248–3250 (1999).
73. Chen, K. C., Wu, J. Y., Yang, W. B. & Hwang, S. C. Evaluation of effective diffusion coefficient and intrinsic kinetic parameters on azo dye biodegradation using PVA-immobilized cell beads. *Biotechnol. Bioeng.* **83**, 821–832 (2003).
74. Winkler, M. K., Kleerebezem, R., Kuenen, J. G., Yang, J. & van Loosdrecht, M. C. Segregation of biomass in cyclic anaerobic/aerobic granular sludge allows the enrichment of anaerobic ammonium oxidizing bacteria at low temperatures. *Environ. Sci. Technol.* **45**, 7330–7337 (2011).
75. Winkler, M. K. et al. Selective sludge removal in a segregated aerobic granular biomass system as a strategy to control PAO-GAO competition at high temperatures. *Water Res.* **45**, 3291–3299 (2011).
76. Chen, K.-C. & Lin, Y.-F. Immobilization of microorganisms with phosphorylated polyvinyl alcohol (PVA) gel. *Enzym. Microb. Technol.* **16**, 79–83 (1994).
77. Wong, P. K. & Chang, L. Effects of copper, chromium and nickel ions on inorganic nitrogen and phosphorus uptake in *Chlorella* species. *Microbios* **67**, 107–115 (1991).
78. Ichimura, K. Effect of poly (ethylene glycol) on the photochemical immobilization of an enzyme in photocrosslinkable poly (vinyl alcohol). *Macromol. Chem. Phys.* **188**, 763–768 (1987).
79. Brányik, T., Kuncová, G., Páca, J. & Demnerová, K. Encapsulation of microbial cells into silica gel. *J. Sol. Gel Sci. Technol.* **13**, 283–287 (1998).
80. Siess, M. & Divies, C. Behaviour of *Saccharomyces cerevisiae* cells entrapped in a polyacrylamide gel and performing alcoholic fermentation. *Eur. J. Appl. Microbiol.* **12**, 10–15 (1981).
81. Lau, P., Tam, N. & Wong, Y. Effect of carrageenan immobilization on the physiological activities of *Chlorella vulgaris*. *Bioresour. Technol.* **63**, 115–121 (1998).
82. Benyahia, F. & Polomarkaki, R. Mass transfer and kinetic studies under no cell growth conditions in nitrification using alginate gel immobilized *Nitrosomonas*. *Process Biochem.* **40**, 1251–1262 (2005).
83. Sliemers, A. O. et al. Completely autotrophic nitrogen removal over nitrite in one single reactor. *Water Res.* **36**, 2475–2482 (2002).
84. French, E., Kozłowski, J. A., Mukherjee, M., Bullerjahn, G. & Bollmann, A. Enrichment and characterization of three ammonia-oxidizing Archaea from freshwater environments. *Appl. Environ. Microbiol.* **78**, 5773–5780 (2012).

## ACKNOWLEDGEMENTS

This work was supported by the Defense Advanced Research Projects Agency [contract number HR0011-17-2-0064] and the U.S. Department of Energy (DOE) [contract number DE-SC0020356]. The author would like to thank Bruce Godfrey for his precious comments on the paper.

## AUTHOR CONTRIBUTIONS

Matthieu Landreau and HeeJun You conceived and carried out the experiments. David A. Stahl and Mari K. H. Winkler supervised the project. Matthieu Landreau wrote the manuscript with support from Mari K. H. Winkler and David A. Stahl.

### COMPETING INTERESTS

The authors declare no competing interests.

### ADDITIONAL INFORMATION

**Correspondence** and requests for materials should be addressed to Matthieu Landreau.

**Reprints and permission information** is available at <http://www.nature.com/reprints>

**Publisher's note** Springer Nature remains neutral with regard to jurisdictional claims in published maps and institutional affiliations.



**Open Access** This article is licensed under a Creative Commons Attribution 4.0 International License, which permits use, sharing, adaptation, distribution and reproduction in any medium or format, as long as you give appropriate credit to the original author(s) and the source, provide a link to the Creative Commons license, and indicate if changes were made. The images or other third party material in this article are included in the article's Creative Commons license, unless indicated otherwise in a credit line to the material. If material is not included in the article's Creative Commons license and your intended use is not permitted by statutory regulation or exceeds the permitted use, you will need to obtain permission directly from the copyright holder. To view a copy of this license, visit <http://creativecommons.org/licenses/by/4.0/>.

© The Author(s) 2021